Cyanide-Bridged W^{V}Mn^{III} Single-Chain Magnet with Isolated Mn^{III} Moieties Exhibiting Two Types of Relaxation Dynamics

Jung Hee Yoon,[†] Jin Wuk Lee,[†] Dae Won Ryu,[†] Sang Yup Choi,[†] Sung Won Yoon,[‡] Byoung Jin Suh,[‡] Eui Kwan Koh,[§] Hyoung Chan Kim,[¶] and Chang Seop Hong*,[†]

[†]Department of Chemistry (BK21), Korea University, Seoul 136-713, Korea
[‡]Department of Physics, The Catholic University of Korea, Buchon 420-743, Korea
[§]Nano-Bio System Research Team, Korea Basic Science Institute, Seoul 136-713, Korea
[¶]National Fusion Research Institute, Daejeon 305-333, Korea

S *Supporting Information*

ABSTRACT: A 5d−3d bimetallic compound was prepared by self-assembling $[W(CN)_8]^{3-}$ and the Mn^{III} Schiff bases. This neutral complex consists of cyanide-linked W^{V}Mn^{III} anionic chains and isolated Mn^{III} Schiff base cations. We demonstrate that two types of relaxation processes are involved in the system; the low-T dynamics may come from magnetic domain dynamics and the high-T relaxation stems from the anionic chain, revealing single-chain magnet character.

Low-dimensional magnetic materials such as single-molecule magnets (SMMs)[1] and single-chain magnets (SCMs)[2] showing slow magnetic relaxation have been explored with great interest because they have unique potential applications for information storage devices. Recently, a new research challenge has arisen because multiple relaxation processes were observed in some SMMs and SCMs. For instance, lanthanide-based SMMs possessing a strong spin−orbital coupling under the crystal fields demonstrated two-step magnetic relaxation processes with high anisotropic barriers.[3] Moreover, the 5f metal-containing single-ion magnet U(H$_2$BPz$_2$)$_3$ [H$_2$BPz$_2$ = dihydrobis(pyrazolylborate)] displayed a secondary slow relaxation process under an external magnetic field.[4] Even the one-dimensional (1D) oxamato-bridged heterobimetallic Cu−Co chain illustrated two relaxation regimes in different temperature regions.[5] Furthermore, a smooth transition from SMM to SCM character upon an applied static field was found in a 1D coordination polymer dysprosium bis(nitronyl nitroxide) accounting for size effects on the dynamic behavior.[6] Thus, such newly emerging phenomena regarding slow relaxation dynamics in SMMs and SCMs have been discovered in the past a few years, which would broaden the territory of molecular magnetism.

Here, we report the synthesis, crystal structure, and magnetic properties of 1D complex [Mn(L)W(CN)$_8$][Mn(L)-(H$_2$O)$_2$]$_2$·MeCN·H$_2$O [**1**·MeCN·H$_2$O; H$_2$L = *N,N′*-bis(2-hydroxynaphthalene-1-carbaldehyde)-1,3-diaminopropane] comprising both bimetallic W^{V}Mn^{III} anionic chains and two isolated Mn^{III} cations. Notably, two types of relaxation processes, which probably originate from the SCM behavior

of the linear chain and a long-range order at low temperatures, are perceivable in this complex.

Compound **1** was obtained by a stoichiometric reaction of Cs$_3$[W(CN)$_8$]·2H$_2$O with the corresponding Mn^{III} Schiff base in a mixed MeOH/MeCN/H$_2$O solvent. In the IR spectra, the CN stretching peaks evident at 2160w and 2141w cm^{-1} for **1**·MeCN·H$_2$O are compared with that (2145w cm^{-1}) for Cs$_3$[W(CN)$_8$]·2H$_2$O. The peak shift toward higher frequencies can be assigned to the coordination of some CN ligands to nearby Mn^{III} ions.[7]

Figure 1 depicts the crystal structure consisting of a 1D linear bimetallic chain with Mn^{III}W^V repeating units linked by cyanide
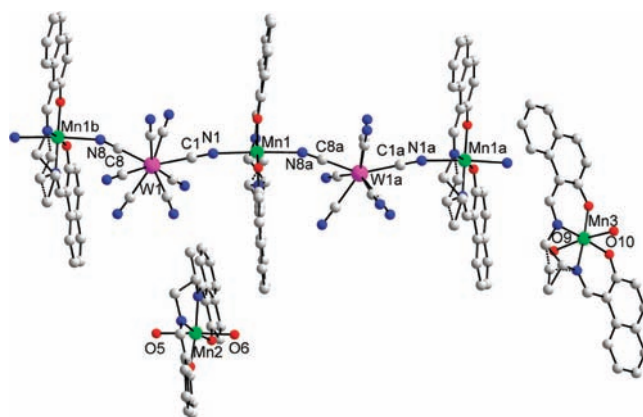

Figure 1. Molecular view of **1**. Symmetry transformations used to generate equivalent atoms: a = x, 1.5 − y, 0.5 + z; b = x, 1.5 − y, −0.5 + z.

bridges and two crystallographically dissimilar Mn^{III} Schiff bases (Mn2 and Mn3). The W−C bond lengths range from 2.142 to 2.181 Å, and the W−C−N angles are slightly away from linearity, with a maximum deviation of 4.2° from 180°.[8] The geometry of the W1 ion surrounded by eight C atoms from the CN groups is determined as a distorted dodecahedron based on the continuous-shape-measure analysis (Table S1 in the Supporting Information, SI).[9] The Mn1 ion is in a tetragonally

elongated octahedral environment, and a typical Jahn−Teller distortion occurs as a result of the longer axial Mn−N bond distances [Mn1−N1 = 2.307(3) Å and Mn1b−N8 = 2.373(4) Å; b = x, 1.5 − y, −0.5 + z] than the averaged equatorial Mn1−N(O) distance of 1.92(5) Å.[8] The Mn−N−C angles in the cyanide-bridging pathways, which are magnetically important, correspond to 166.2(3)° for Mn1−N1−C1 and 159.1(4)° for Mn1b−N8−C8. The W−Mn distances within a chain are almost identical, 5.579 Å for Mn1−W1 and 5.605 Å for Mn1−W1a (a = x, 1.5 − y, 0.5 + z). The Mn2 and Mn3 centers are encircled by N_2O_2 donors of the Schiff bases and two O atoms from end-capped water molecules. The axial Mn−O distances are larger than the equatorial ones, spanning from 2.229 to 2.284 Å. This structural feature evidence the occurrence of a Jahn−Teller effect. The intermetallic distances between Mn atoms in the monomers and magnetic ions in the chain are 9.933 Å for Mn2−W1 and 8.533 Å for Mn3−Mn1a. In the extended structural view (Figures S1−S4 in the SI), the Mn monomers (Mn2 and Mn3) are well separated by the existence of 1D octacyanometalate-based $W^V Mn^{III}$ linear chains.

The thermal variation of the magnetic susceptibility data for 1·MeCN·H$_2$O was recorded at 1000 G (Figure S5 in the SI). The $\chi_m T$ value of 8.91 cm^3 K mol^{-1} at 300 K, somewhat smaller than the spin-only value of 9.38 cm^3 K mol^{-1} for three uncoupled Mn^{III} ions ($S_{Mn} = 2$) and one W^V ion ($S_W = {}^1/_2$), decreases smoothly and then abruptly upon cooling. This behavior supports the presence of antiferromagnetic couplings among paramagnetic W and Mn centers. To probe the underlying magnetic exchange characteristics, the Seiden chain model (χ_{chain}) based on $\mathbf{H} = -2J\sum_i (S_{W,i} \cdot S_{Mn,i} + S_{W,i} \cdot S_{Mn,i+1})$ for the $(2, {}^1/_2)$ alternating spin-chain system was employed[10] and two isolated paramagnetic Mn^{III} subunits ($2\chi_{Mn}$) were also included in the fitting process. The overall equation of $\chi_m = \chi_{chain} + 2\chi_{Mn}$ was utilized under consideration of the molecular field approximation (zj') to fit the data at $T > 7$ K, and a best result gives parameters of $g = 1.96$, $J = -5.1$ cm^{-1}, and $zj' = -0.10$ cm^{-1}. It is manifest that intrachain antiferromagnetic couplings ($J < 0$) are communicated between Mn^{III} and W^V spins through cyanides. To gain insight into the magnetic exchange mechanism, we carried out density functional theory calculations on the dodecahedral [W-(CN)$_8$]$^{3-}$ (Figure S6 in the SI). From the results, the N ends of bridging CN ligands are positioned at A and B sites at the same time.[11] The spin density of the W center can be delocalized over the N ends in a π type. The N p$_\pi$ orbitals dominantly overlap with d$_\pi$ magnetic orbitals of neighboring Mn ions, eventually leading to the apparent antiferromagnetic arrangements. The saturation magnetization per Mn$_3$W in the $M(H)$ data taken at 2 and 4 K (Figure S7 in the SI) is equal to 9.03 Nβ, lower than the theoretical result of $g(S_{Mn} - S_W + 2S_{Mn}) = 11$ Nβ, assuming $g = 2$. This disparity may be due to the intermolecular antiferromagnetic interactions and magnetic anisotropy of the system.[7,8] The critical field of $H_C = 1000$ G was determined by the peak in the derivative of magnetization at 2 K. This behavior complies with the $\chi_m(T)$ curves, where the cusp at 3 K is present below H_C and absent above H_C (Figure S8 in the SI). This observation is diagnostic of a field-induced metamagnetic transition.[8a,10b] In the zero-field-cooled and field-cooled magnetizations, there is an irreversibility, indicating the presence of a magnetic phase (Figure S9 in the SI).

The spin dynamics was checked by measuring the alternating-current (ac) magnetic susceptibility of 1·MeCN·

H$_2$O at $H_{dc} = 0$ G (where dc is direct current), $H_{ac} = 5$ G, and several oscillating frequencies (f; Figures 2a and S10 in the SI).
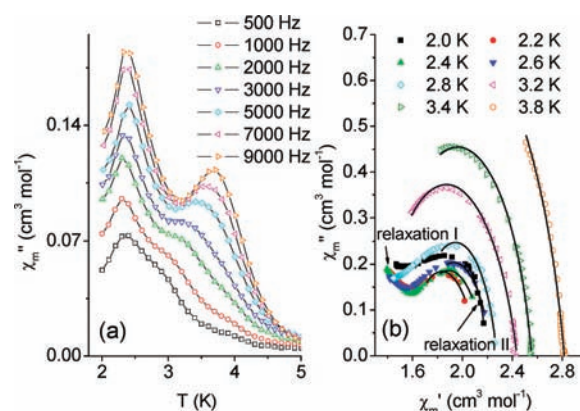

Figure 2. (a) Temperature dependence of χ_m'' for 1·MeCN·H$_2$O at zero dc field and an ac field of 5 G with the indicated frequencies. The lines are guides for the eye. (b) Cole−Cole plots for 1·MeCN·H$_2$O. The solid lines represent the fit with the generalized Debye model.

A peak at $T_p = 2.3$ K and a shoulder at ~2.7 K are observed in the out-of-phase (χ_m'') plot at $f = 500$ Hz. The shoulder signal moves toward higher temperatures with increasing f, characteristic of slow magnetic relaxation, while the lower peak lingers around the same temperature, indicating the onset of a long-range ordering. The heat capacity measurement should be convincing evidence for low-temperature long-range order. In the Cole−Cole diagrams (Figures 2b and S11 in the SI), there is the distinct onset of a faster relaxation (relaxation I) and a slower relaxation (relaxation II) in the low-T regime ($T \leq 2.8$ K) as well as the single relaxation region (relaxation II) in the high-T regime ($T \geq 3.2$ K). In the low-T region around T_p, the faster relaxation may arise from the presence of isolated Mn^{III} ions or a fast domain response due to the long-range order. Because SMM behavior was demonstrated only in some Mn^{III} dimers (not monomers), it is probable that the latter is responsible for the relaxation.[12]

To analyze the relaxation process, it was fitted using the generalized Debye model, where α gauges the distribution width of single relaxation processes and lies between 0 and 1 (Table S2 in the SI).[3e,13] The well-fitted small α value of less than 0.34 at the slow relaxation region indicates a distribution of relaxation times. The relaxation II can be attributed to the SCM dynamics of the W^{V}Mn^{III} skeleton because the anisotropic 1D magnetic trait is defined by the combination of not only the effect of single-ion anisotropy from the Jahn−Teller ion but also an intrachain magnetic coupling contribution.[14] The peak shift in the ac signals was taken into account with a quantity of $\varphi = \Delta T_p / [T_p \Delta(\log f)]$. The φ value amounts to 0.28, which is in the range of superparamagnets.[1,2] Using the Arrhenius equation of $\tau = \tau_0 \exp(\Delta_\tau / kT)$, where τ is equal to $1/2\pi f$ and Δ_τ is the activation energy, the best parameters of $\tau_0 = 9.42 \times 10^{-9}$ s and $\Delta_\tau/k = 19.3$ cm^{-1} are acquired (Figure S12 in the SI). As expected from the Glauber model in a 1D anisotropic system,[2i] a linear fit in the $\ln(\chi_m' T)$ versus $1/T$ plot affords $\Delta_\xi = 1.1$ cm^{-1} on the basis of the magnetic expression of $\chi T \propto \exp(\Delta_\xi/kT)$ where Δ_ξ is the energy barrier to create a domain wall in the chain (Figure S13 in the SI). The maximum in the curve is relevant with finite-size effects owing to the presence of defects and intermolecular

antiferromagnetic interactions. Similar examples containing the W−Mn chains were reported to show typical SCM character.[2d,8]

To further examine the relaxation dynamics, we measured ac data with increasing magnetic field (Figures S14 and S15 in the SI). The Cole−Cole plots at $T = 2.0$ K show that relaxation I is predominantly appreciable until $H = 500$ G and the tail of relaxation II appears at $H = 800$ G. At $T = 2.4$ K, both relaxations I and II are detectable and relaxation II is more evident at $H = 800$ G. When the temperature increases to $T = 2.8$ K, relaxation II is prevalent. Thus, the application of an external field affects the spin dynamics for relaxations I and II. At $T = 3.2$ K in the relaxation II region, the shape of the Cole−Cole plots remains semicircular until $H = 800$ G and then disappears, which contrasts with the low-T domains. The larger magnetic fields ($H > 800$ G) mostly suppress the slow relaxation processes in the wake of a field-induced magnetic ordering, as confirmed by the temperature dependence of ac susceptibilities at $H = 3000$ G (Figure S16 in the SI) in which the peak position at 3.1 K is frequency-independent and attributed to an ordering temperature.

To understand the in-depth magnetic nature of **1**, a dehydrated compound $[Mn(L)W(CN)_8][Mn(L)]_2$ (**1a**) was obtained by the procedure in which $\mathbf{1}\cdot MeCN\cdot H_2O$ was heated at 140 °C under N_2 flow because solvent molecules were thermally decomposed at 130 °C (Figure S17 in the SI). The Nujol IR data (Figure S18 in the SI) disclose that water molecules are completely removed for **1a** and powder X-ray diffraction data were obtained (Figure S19 in the SI). The $\chi_m T(T)$ curve of **1a** is quite different from that for $\mathbf{1}\cdot MeCN\cdot H_2O$, which may originate from the pronounced magnetic couplings between W^V and Mn^{III} of the desolvated sample generated by the removal of solvent molecules (Figure S5 in the SI). The field- and temperature-dependent curves for **1a** indicate operation of antiferromagnetic interactions and no magnetic order (Figures S20 and 21 in the SI). From the ac data with and without dc fields (Figures S22−24 in the SI), the slow magnetic relaxation processes are largely quelled in **1a**, which may be due to the structural variation and subsequent magnetic consequence caused by solvent removal.

In summary, we have prepared a new bimetallic 3d−5d compound **1** composed of the $W^V Mn^{III}$ anionic chain and isolated Mn^{III} cationic moieties. This material shows two types of relaxation domains associated with SCM character and long-range ordering.

ASSOCIATED CONTENT

Ⓢ Supporting Information

X-ray crystallographic files in CIF format, detailed preparations, and additional structural and magnetic data. This material is available free of charge via the Internet at http://pubs.acs.org.

AUTHOR INFORMATION

Corresponding Author

*E-mail: cshong@korea.ac.kr.

ACKNOWLEDGMENTS

REFERENCES

(1) (a) Sessoli, R.; Gatteschi, D.; Caneschi, A.; Novak, M. A. *Nature* **1993**, *365*, 141. (b) Leuenberger, M. N.; Loss, D. *Nature* **2001**, *410*, 789. (c) Wernsdorfer, W.; Aliaga-Alcalde, N.; Hendrickson, D. N.; Christou, G. *Nature* **2002**, *416*, 406. (d) Wernsdorfer, W.; Sessoli, R. *Science* **1999**, *284*, 133. (e) Jiang, S.-D.; Wang, B.-W.; Su, G.; Wang, Z.-M.; Gao, S. *Angew. Chem., Int. Ed.* **2010**, *49*, 7448.

(2) (a) Clérac, R.; Miyasaka, H.; Yamashita, M.; Coulon, C. *J. Am. Chem. Soc.* **2002**, *124*, 12837. (b) Bogani, L.; Sangregorio, C.; Sessoli, R.; Gatteschi, D. *Angew. Chem., Int. Ed.* **2005**, *44*, 5817. (c) Bogani, L.; Vindigni, A.; Sessolia, R.; Gatteschi, D. *J. Mater. Chem.* **2008**, *18*, 4750. (d) Choi, S. W.; Kwak, H. Y.; Yoon, J. H.; Kim, H. C.; Koh, E. K.; Hong, C. S. *Inorg. Chem.* **2008**, *47*, 10214. (e) Ferbinteanu, M.; Miyasaka, H.; Wernsdorfer, W.; Nakata, K.; Sugiura, K.; Yamashita, M.; Coulon, C.; Clérac, R. *J. Am. Chem. Soc.* **2005**, *127*, 3090. (f) Harris, T. D.; Bennett, M. V.; Clérac, R.; Long, J. R. *J. Am. Chem. Soc.* **2010**, *132*, 3980. (g) Sun, H.-L.; Wang, Z.-M.; Gao, S. *Coord. Chem. Rev.* **2010**, *254*, 1081. (h) Yoon, J. H.; Ryu, D. W.; Kim, H. C.; Yoon, S. W.; Suh, B. J.; Hong, C. S. *Chem.—Eur. J.* **2009**, *15*, 3661. (i) Coulon, C.; Miyasaka, H.; Clérac, R. *Struct. Bonding (Berlin)* **2006**, *122*, 163.

(3) (a) Guo, Y.-N.; Xu, G.-F.; Gamez, P.; Zhao, L.; Lin, S.-Y.; Deng, R.; Tang, J.; Zang, H.-J. *J. Am. Chem. Soc.* **2010**, *132*, 8538. (b) Hewitt, I. J.; Tang, J.; Madhu, N. T.; Anson, C. E.; Lan, Y.; Luzon, J.; Etienne, M.; Sessoli, R.; Powell, A. K. *Angew. Chem., Int. Ed.* **2010**, *49*, 6352. (c) Jiang, S.-D.; Wang, B.-W.; Sun, H.-L.; Wang, Z.-M.; Gao, S. *J. Am. Chem. Soc.* **2011**, *133*, 4730. (d) Guo, Y.-N.; Xu, G.-F.; Wernsdorfer, W.; Ungur, L.; Guo, Y.; Tang, J.; Zhang, H.-J.; Chibotaru, L. F.; Powell, A. K. *J. Am. Chem. Soc.* **2011**, *133*, 11948. (e) Car, P.-E.; Perfetti, M.; Mannini, M.; Favre, A.; Caneschi, A.; Sessoli, R. *Chem. Commun.* **2011**, *47*, 3751.

(4) Rinehart, J. D.; Meihaus, K. R.; Long, J. R. *J. Am. Chem. Soc.* **2010**, *132*, 7572.

(5) Ferrando-Soria, J.; Pardo, E.; Ruiz-García, R.; Cano, J.; Lloret, F.; Julve, M.; Journaux, Y.; Pasán, J.; Ruiz-Pérez, C. *Chem.—Eur. J.* **2011**, *17*, 2176.

(6) Liu, R.; Li, L.; Wang, X.; Yang, P.; Wang, C.; Liao, D.; Sutter, J.-P. *Chem. Commun.* **2010**, *46*, 2566.

(7) (a) Przychodzeń, P.; Rams, M.; Guyard-Duhayon, C.; Sieklucka, B. *Inorg. Chem. Commun.* **2005**, *8*, 350. (b) Kou, H.-Z.; Ni, Z.-H.; Zhou, B. C.; Wang, R.-J. *Inorg. Chem. Commun.* **2004**, *7*, 1150. (c) Przychodzeń, P.; Lewiński, K.; Balanda, M.; Pelka, R.; Rams, M.; Wasiutyński, T.; Guyard-Duhayon, C.; Sieklucka, B. *Inorg. Chem.* **2004**, *43*, 2967. (d) Ko, H. H.; Lim, J. H.; Yoo, H. S.; Kang, J. S.; Kim, H. C.; Koh, E. K.; Hong, C. S. *Dalton Trans.* **2007**, 2061.

(8) (a) Choi, S. W.; Ryu, D. W.; Lee, J. W.; Yoon, J. H.; Kim, H. C.; Lee, H.; Cho, B. K.; Hong, C. S. *Inorg. Chem.* **2009**, *48*, 9066. (b) Yoo, H. S.; Ko, H. H.; Ryu, D. W.; Lee, J. W.; Yoon, J. H.; Lee, W. R.; Kim, H. C.; Koh, E. K.; Hong, C. S. *Inorg. Chem.* **2009**, *48*, 5617.

(9) (a) Llunell, M.; Casanova, D.; Cirera, J.; Bofill, J. M.; Alemany, P.; Alvarez, S.; Pinsky, M.; Avnir, D. *SHAPE: Continuous shape measures of polygonal and polyhedral molecular fragments*, version 1.1b; University of Barcelona: Barcelona, 2005. (b) Cirera, J.; Ruiz, E.; Alvarez, S. *Chem.—Eur. J.* **2006**, *12*, 3162.

(10) (a) Seiden, J. *J. Phys. Lett.* **1983**, *44*, L947. (b) Harris, T. D.; Coulon, C.; Clérac, R.; Long, J. R. *J. Am. Chem. Soc.* **2011**, *133*, 123.

(11) Visinescu, D.; Desplanches, C.; Imaz, I.; Bahers, V.; Pradhan, R.; Villamena, F. A.; Guionneau, P.; Sutter, J.-P. *J. Am. Chem. Soc.* **2006**, *128*, 10202.

(12) Miyasaka, H.; Saitoh, A.; Abe, S. *Coord. Chem. Rev.* **2007**, *251*, 2622.

(13) Cole, K. S.; Cole, R. H. *J. Chem. Phys.* **1941**, *9*, 341.

(14) Bogani, L.; Vindigni, A.; Sessoli, R.; Gatteschi, D. *J. Mater. Chem.* **2008**, *18*, 4750.